

Precise Fabrication and Manipulation of Individual Polymer Nanofibers

Daewon Kim, Byeong Jun Cha, Hua Guo, Guanhui Gao, Chris Pennington, Michael S. Wong, Bezawit A. Getachew, and Yimo Han*



Cite This: *Nano Lett.* 2024, 24, 6038–6042



Read Online

ACCESS |

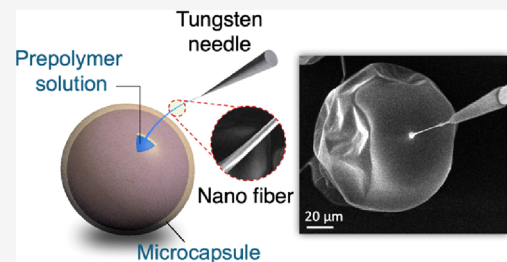
Metrics & More

Article Recommendations

Supporting Information

ABSTRACT: Polymer nanofibers hold promise in a wide range of applications owing to their diverse properties, flexibility, and cost effectiveness. In this study, we introduce a polymer nanofiber drawing process in a scanning electron microscope and focused ion beam (SEM/FIB) instrument with *in situ* observation. We employed a nanometer-sharp tungsten needle and prepolymer microcapsules to enable nanofiber drawing in a vacuum environment. This method produces individual polymer nanofibers with diameters as small as \sim 500 nm and lengths extending to millimeters, yielding nanofibers with an aspect ratio of 2000:1. The attachment to the tungsten manipulator ensures accurate transfer of the polymer nanofiber to diverse substrate types as well as fabrication of assembled structures. Our findings provide valuable insights into ultrafine polymer fiber drawing, paving the way for high-precision manipulation and assembly of polymer nanofibers.

KEYWORDS: polymer, nanofiber, microcapsule, fiber drawing, SEM, FIB



Polymer fibers are extensively utilized in textile applications. Recent advancements in ultrafine polymer fibers have expanded their potential applications, including tissue engineering and filtration membranes, due to their attributes such as low cost, light weight, high flexibility, and ease of structural and surface manipulation.^{1–3} The synthesis of ultrafine polymer fibers is predominantly achieved through top-down methods such as electrospinning^{4,5} and solution blow spinning.⁶ These techniques enable the mass production of polymer fibers with significant surface area and porosity, suitable for biomedical and membrane applications. However, the limited control over individual polymer fibers poses a constraint for these top-down approaches in electronic device applications.

Fiber drawing from viscous liquids offers a method to produce individual fibers.⁷ Conventional fiber drawing has been widely employed in the production of optical fibers for decades.⁸ Recent advancements demonstrate the promising potential of thermally drawn polymer fibers as building blocks for various device applications.⁹ Nonetheless, the fiber size using this method remains in the range of hundreds of micrometers. Although researchers have reported the drawing of polyaniline nanowires using a sharp scanning tunneling microscope (STM) tip, resulting in stretching to approximately 50 nm in length, the challenges associated with visualizing and manipulating these polymer nanowires limit their fundamental investigation and practical applications. Here, we present a new process for drawing polymer nanofibers employing a nanometer-sharp tungsten needle and encapsulated prepolymer solution (Figure 1a). This method enables precise fabrication and manipulation

of long-aspect-ratio polymer nanofibers while offering the capability for *in situ* imaging of the entire process.

The fiber drawing and *in situ* nanoscale imaging are facilitated by a scanning electron microscope and focused ion beam (SEM/FIB) instrument operated within a vacuum environment. We utilize polyurethane to construct a microcapsule structure encapsulating the prepolymer solution for nanofiber drawing (Figure S1). The microcapsule shell is \sim 1 micrometer thick. While the mechanical strength of polyurethane adequately withstands the pressure difference in a vacuum environment (Figure 1b), the polymer microcapsules prevent the evaporation of solvent from the prepolymer solution. Through this approach, we can access fresh prepolymer solution with the desired viscosity within the SEM/FIB instrument using a fiber drawing needle (Figure 1c).

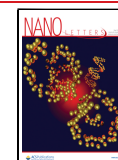
To demonstrate our approach, we utilize isophorone diisocyanate (IPDI) dissolved in chlorobenzene as the prepolymer material.^{11,12} IPDI is a small molecule and undergoes polymerization in the presence of a sufficient amount of water. Upon exposure to air, it partially oligomerizes, forming dimers, trimers, and larger oligomers (Figure S2). During the fabrication of polyurethane microcapsules, IPDI is exposed to a

Received: February 14, 2024

Revised: May 7, 2024

Accepted: May 8, 2024

Published: May 12, 2024



ACS Publications

© 2024 American Chemical Society

6038

<https://doi.org/10.1021/acs.nanolett.4c00799>
Nano Lett. 2024, 24, 6038–6042

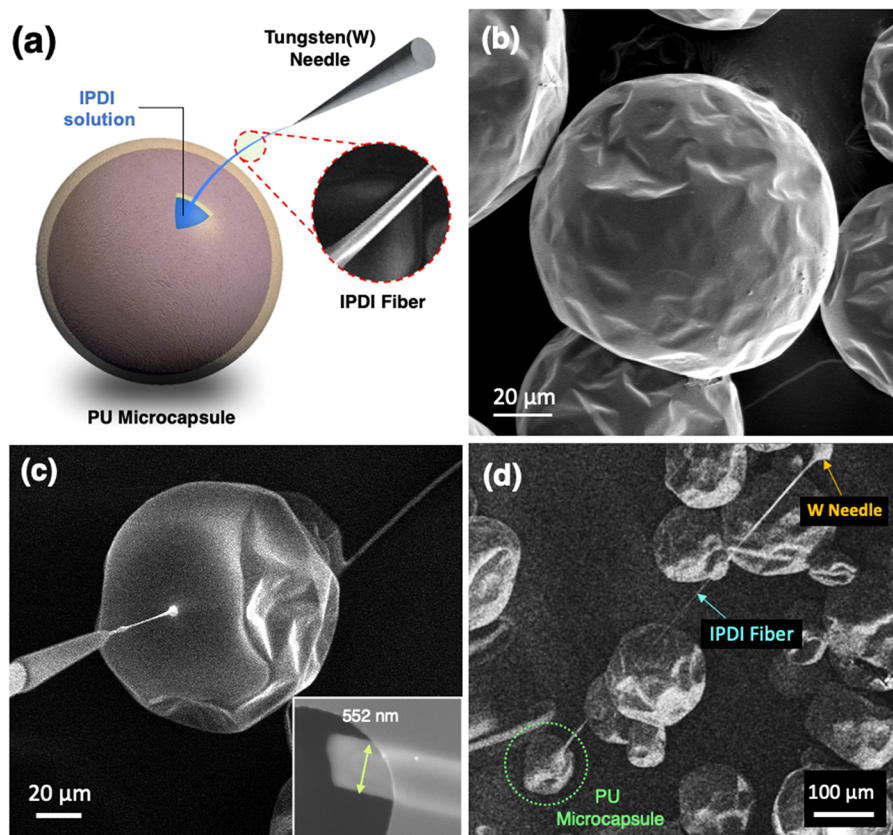


Figure 1. Fabrication of polymer nanofibers. (a) Schematic illustrating the process for generating nanofibers using a sharp tungsten needle. (b) SEM image of polyurethane microcapsule encapsulated IPDI oligomer solution, maintained in a vacuum environment without leakage. (c) SEM image of a polymer nanofiber at the initiation of the drawing process. Inset: TEM image of the tip of a nanofiber. (d) SEM image of an ultralong nanofiber drawn from the microcapsule.

high-humidity environment, facilitating the formation of oligomers. Therefore, the prepolymer material within the microcapsule will likely consist of IPDI oligomers in chlorobenzene solvent (more evidence is presented later in the manuscript).^{13,14}

We employed the sharp tungsten needle of the manipulator within the SEM/FIB system to draw the nanofibers. The tungsten needle possesses a sharp tip approximately 200 nm in size (Figure S3) and precise movement with a minimum 50 nm step size in all three dimensions. This facilitates the accurate approach of individual microcapsules to access the prepolymer solution. In addition, *in situ* SEM imaging enables high-resolution videos to monitor the movement of the tungsten needle and the entire stretching process of the nanofibers.

During SEM recording, we utilized the needle to puncture the microcapsule, breaking it and allowing the prepolymer solution to be released and saturate the surface of the microcapsule (Supplementary Movie 1). At this stage, the needle comes into contact with a fresh prepolymer solution. Subsequently, we retracted the needle slowly from the microcapsule, observing the formation of a thin nanowire connecting the microcapsule and the tungsten needle (Figure 1c). The size of the fiber is considerably smaller than that of the microcapsule. The narrowest width of the wire observed is 550 nm (inset of Figure 1c). Moreover, as we continue to draw the nanofiber gradually, we notice that this approach also yields ultralong fibers, extending up to a millimeter scale (Figure 1d, Supplementary Movie 2). Ultimately, the fiber breaks at a thin point once the nanowire solidifies and ceases to stretch.

Given the crucial role of prepolymer solution viscosity in fiber drawing,⁷ we test the nanofiber drawing under identical drawing conditions with varying viscosity. As IPDI oligomers are much more viscous than the solvent, which is chlorobenzene, viscosity control is achieved by adjusting the concentration of chlorobenzene. We observed that at higher viscosity (12.5 wt % chlorobenzene), fibers solidify more rapidly, leading to premature breakage and cessation of fiber stretching (Figure 2a). The breakage point exhibits a blunt profile (inset of Figure 2a). Conversely, lower viscosity with 25 wt % chlorobenzene results in consistent, prolonged nanofiber formation during our drawing process (Figure 2b). Further viscosity reduction produces much thinner junctions between the needle and the prepolymer solution, causing breakage with sharply tipped gaps (Figure 2c). These findings suggest an optimized viscosity for consistent nanofiber drawing in this process.

Following the solidification of the long nanofiber, we can detach the fiber from the microcapsule by either rapid direct pulling or ion beam cutting. Upon breakage, the fiber remains fully attached to the tungsten needle manipulator and can be accurately transferred to another substrate. To demonstrate this feasibility, we transfer our nanofiber onto a transmission electron microscope (TEM) grid mounted on the SEM/FIB stage (Figure 3a). We observe that the prepolymer solution attached to the tungsten needle is not fully solidified inside owing to the formation of a solid shell. By applying a slight pressure at the tungsten needle tip, the nanofiber detaches from the needle tip and adheres well to the amorphous carbon film on the TEM grid (Figure 3b). Subsequently, we can remove the

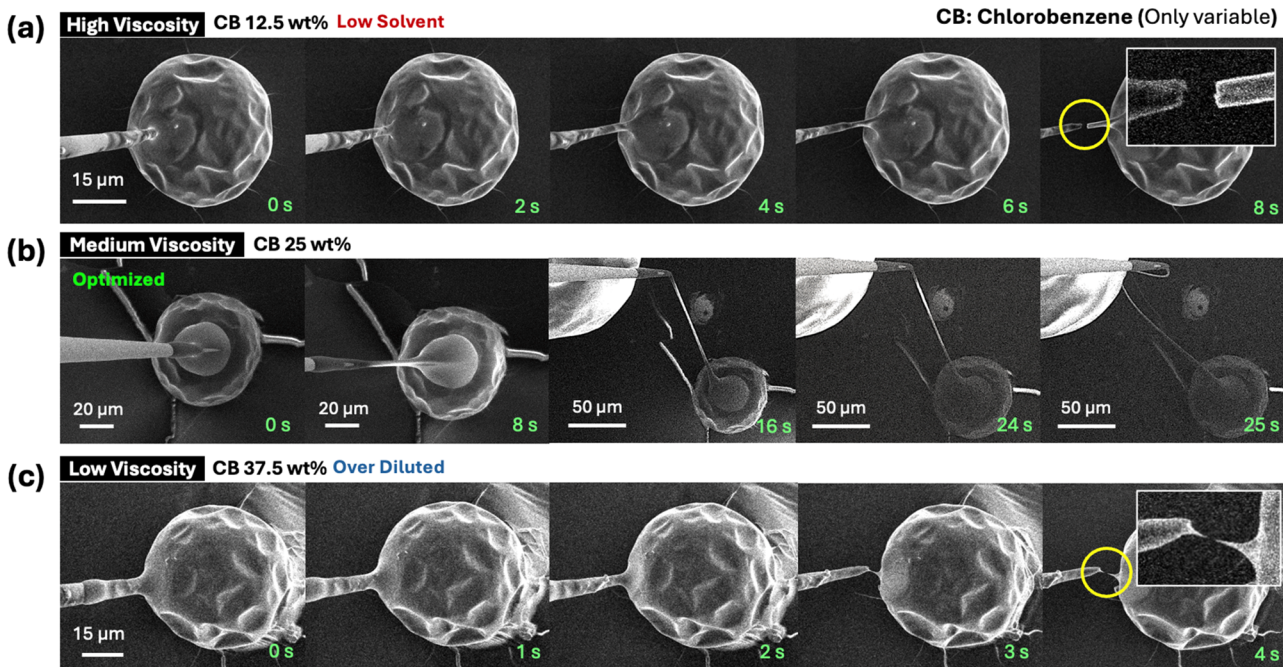


Figure 2. *In situ* SEM imaging of nanofibers with varying prepolymer solution viscosities. Nanofiber drawing from IPDI monomer solution with different solvent concentrations (chlorobenzene) of 12.5 wt % (a), 25 wt % (b), and 37.5 wt % (c), respectively. The optimized chlorobenzene concentration is 25 wt %. The fracture differences are highlighted by yellow circles, with zoomed-in images shown in the insets in (a) and (c).

needle from the TEM grid, while the nanofiber remains on the TEM grid (Figure 3c). We observed precise positioning of the fiber without obvious drift in SEM images. This transfer method can be extended to other substrates such as silicon wafers and polydimethylsiloxane (PDMS).

Transferring the nanofiber onto a TEM grid enables us to characterize its structure with higher resolution using high-angle annular dark field scanning transmission electron microscopy (HAADF-STEM) (Figure 3d and Figure S4). The width of the nanofiber is observed to be around hundreds of nanometers. Selected area electron diffraction (SAED) reveals that the solidified nanofiber exhibits a completely amorphous structure, as anticipated (inset of Figure 3d). The nanofiber remains stably attached to the TEM grid throughout the loading/unloading process and under the influence of the high-energy electron beam, suggesting strong adhesion of the nanofiber to the substrate. In addition to precise transfer, we can also achieve precise assembly of the polymer nanofibers by using the tungsten manipulator. We opt to break the nanofiber after solidification in the middle and then utilize the tungsten manipulator to bring the halves of the nanofiber into contact, creating an interlacing connection (Figure S5 and Supplementary Movie 3). The nanofibers intersect and slowly deform, resulting in a twisted structure (Figure 3e). This suggests a propensity for the nanofibers to form twisted junctions, possibly due to electrostatic interactions. This observation demonstrates the potential of our approach to create specific geometries for polymer nanofiber assembly while enabling high-resolution *in situ* imaging simultaneously.

The nanofibers and their assemblies unloaded from the SEM/FIB instrument consist of solidified IPDI oligomers. To enhance the polymerization of the IPDI nanofibers, we apply sufficient water treatment to fully polymerize the nanofibers (Figure S6). After water treatment, we perform more TEM imaging and observe no obvious morphology change in the nanofiber (Figure S7). To verify the polymerization of the solidified nanofiber

through the water treatment process, we employ Fourier transform infrared (FT-IR) and X-ray photoelectron spectroscopy (XPS) to compare the chemical bonding environments before and after treatment. We also perform mass spectrometry (MS) to understand the molecular weights. However, these methods cannot be directly applied to the nanofiber due to its small size. Therefore, we prepare equivalent bulk solidified prepolymer material that has undergone a process similar to that for the nanofibers (Figure S8). With this sample, we compare the chemical composition at each stage of the reaction: the as-received monomer solution, the air-exposed and solidified sample, and the water-treated polymerized material (Figure 4a).

Based on the FT-IR results, as-received IPDI monomers exhibit a single strong peak at 2250 cm^{-1} , corresponding to $\text{N}=\text{C}=\text{O}$ stretching,¹⁵ while samples after solidification display additional features originating from C–N stretching of amine ($1020\text{--}1200\text{ cm}^{-1}$) and N–H wagging of secondary amine ($750\text{--}900\text{ cm}^{-1}$).¹⁶ (Figure 4b). Various FT-IR measurements taken from different locations on the solidified sample suggest oligomerization across the sample despite spatial variations (Figure S9). This oligomerization is further confirmed by MS analysis (Figure S10).

Upon the water treatment process, IR absorption at $750\text{--}1200\text{ cm}^{-1}$ increased significantly (Figure 4b), supporting the formation of a suggested polyurea structure. Little formation of the N–H bending feature in the range of $1580\text{--}1650\text{ cm}^{-1}$ indicates the lack of primary amine, suggesting the formation of a secondary-amine-rich polyurea structure. In addition, N 1s XPS reveals an additional feature formed with a lower binding energy upon the water treatment (Figure S11), indicating formation of amine groups within the polymerized sample.^{17,18} These observations confirm an effective polymerization process and a greater formation of polyurea structures upon treatment of solidified oligomers with water. Similar results were consistently obtained across multiple samples with analysis of water-treated polymerized samples (Figure S11).

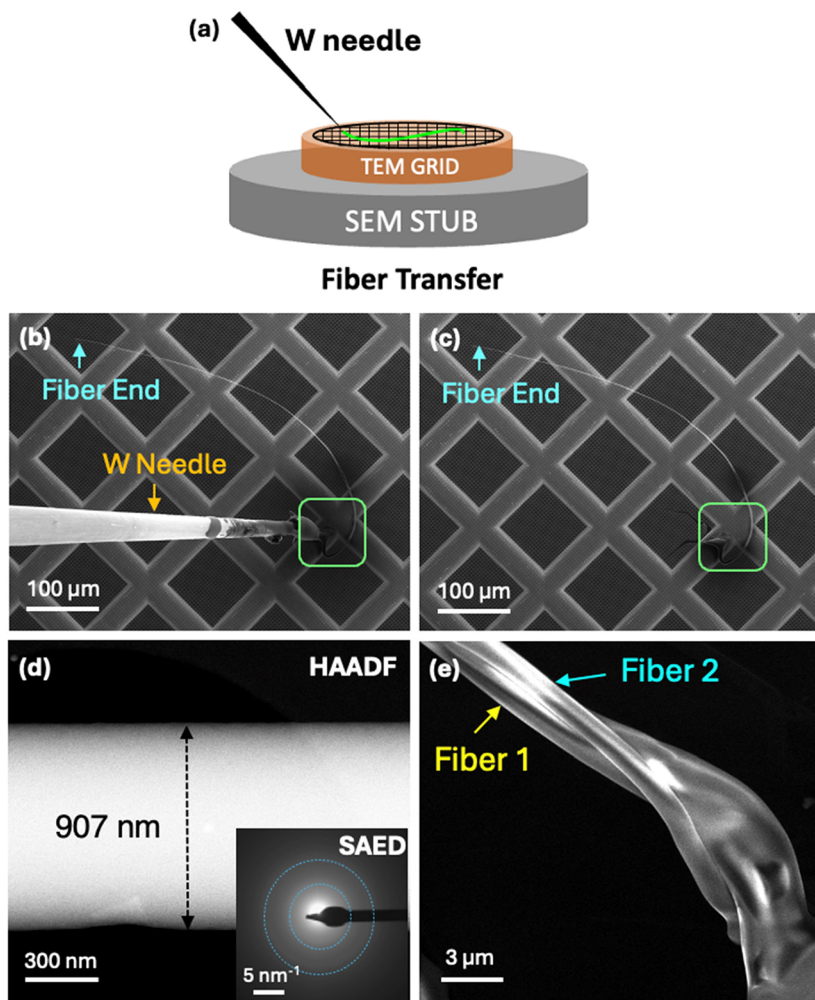


Figure 3. Transfer and assembly of nanofibers. (a) Schematic illustrating the transfer of fibers to a substrate. (b) SEM image of the transfer of a fiber to a TEM grid using the tungsten needle. (c) SEM image of the same area as in (b) after retracting the tungsten needle. (d) HAADF-STEM image of the nanofiber, with SAED in the inset. Dotted circles represent the amorphous rings. (e) SEM image of two fibers assembled to form a twist structure.

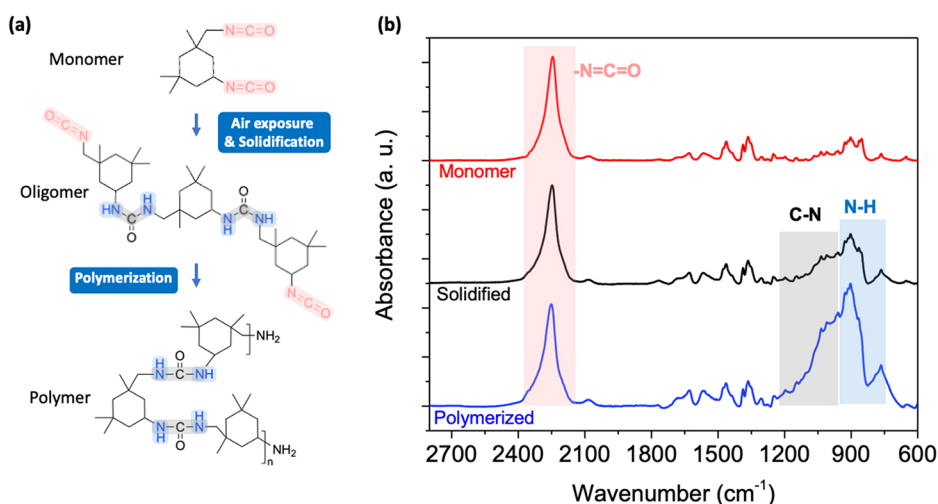


Figure 4. Chemical reactions during nanofiber fabrication. (a) Schematic of the chemical reactions with chemical structures of IPDI monomers, oligomers/prepolymers, and polyurea/polymers. (b) FT-IR spectra of as-received monomers, solidified oligomers, and water-treated polyurea.

In summary, we demonstrate the utilization of the SEM/FIB instrument with a tungsten manipulator to draw nanofibers from encapsulated prepolymer solutions. This approach enables *in situ* high-resolution imaging of the fiber drawing process, precise

manipulation of the solidified nanofibers, and transfer of individual nanofibers to various substrates. The results presented here lay the groundwork for more detailed investigations of the properties of individual nanofibers and

their assembled structures. Moreover, our microcapsule strategy expands the application of the SEM/FIB instrument in polymer sciences, allowing nanoscale fabrication and manipulation of soft materials.

■ ASSOCIATED CONTENT

SI Supporting Information

The Supporting Information is available free of charge at <https://pubs.acs.org/doi/10.1021/acs.nanolett.4c00799>.

Details for methods and materials and additional experimental results ([PDF](#))

In situ movie showing the direct drawing of nanofibers from a microcapsule ([MOV](#))

In situ movie showing the generation of ultralong nanofibers ([AVI](#))

In situ manipulation and twisting of two nanofibers ([MOV](#))

■ AUTHOR INFORMATION

Corresponding Author

Yimo Han — Department of Materials Science and NanoEngineering and Department of Chemistry, Rice University, Houston, Texas 77005, United States;  orcid.org/0000-0003-0563-4611; Email: yh76@rice.edu

Authors

Daewon Kim — Department of Materials Science and NanoEngineering, Rice University, Houston, Texas 77005, United States

Byeong Jun Cha — Department of Chemical and Biomolecular Engineering, Rice University, Houston, Texas 77005, United States

Hua Guo — Shared Equipment Authority, Rice University, Houston, Texas 77005, United States

Guanhui Gao — Department of Materials Science and NanoEngineering and Shared Equipment Authority, Rice University, Houston, Texas 77005, United States

Chris Pennington — Shared Equipment Authority, Rice University, Houston, Texas 77005, United States

Michael S. Wong — Department of Materials Science and NanoEngineering, Department of Chemical and Biomolecular Engineering, Department of Civil and Environmental Engineering, and Department of Chemistry, Rice University, Houston, Texas 77005, United States;  orcid.org/0000-0002-3652-3378

Bezawit A. Getachew — Department of Civil and Environmental Engineering, Rice University, Houston, Texas 77005, United States;  orcid.org/0000-0002-6757-5947

Complete contact information is available at:

<https://pubs.acs.org/doi/10.1021/acs.nanolett.4c00799>

Notes

The authors declare no competing financial interest.

■ ACKNOWLEDGMENTS

The authors acknowledge the support from NSF CAREER (CMMI-2239545), Welch Foundation (C-2065), American Chemical Society Petroleum Research Fund (67236-DNI10), and NSF (CBET-2201361).

■ REFERENCES

- Chen, C.; Feng, J.; Li, J.; Guo, Y.; Shi, X.; Peng, H. Functional Fiber Materials to Smart Fiber Devices. *Chem. Rev.* **2023**, *123* (2), 613–662.
- Zeng, K.; Shi, X.; Tang, C.; Liu, T.; Peng, H. Design, Fabrication and Assembly Considerations for Electronic Systems Made of Fibre Devices. *Nat. Rev. Mater.* **2023**, *8*, 1–10.
- Park, J. H.; Rutledge, G. C. 50th Anniversary Perspective: Advanced Polymer Fibers: High Performance and Ultrafine. *Macromolecules* **2017**, *50* (15), 5627–5642.
- Bhardwaj, N.; Kundu, S. C. Electrospinning: A Fascinating Fiber Fabrication Technique. *Biotechnol. Adv.* **2010**, *28* (3), 325–347.
- Li, D.; Xia, Y. Electrospinning of Nanofibers: Reinventing the Wheel? *Adv. Mater.* **2004**, *16* (14), 1151–1170.
- Daristotle, J. L.; Behrens, A. M.; Sandler, A. D.; Kofinas, P. A Review of the Fundamental Principles and Applications of Solution Blow Spinning. *ACS Appl. Mater. Interfaces* **2016**, *8* (51), 34951–34963.
- Denn, M. M. Continuous Drawing of Liquids to Form Fibers. *Annu. Rev. Fluid Mech.* **1980**, *12* (1), 365–387.
- Talataisong, W.; Ismael, R.; Sandoghchi, S. R.; Rutirawut, T.; Topley, G.; Beresna, M.; Brambilla, G. Novel Method for Manufacturing Optical Fiber: Extrusion and Drawing of Microstructured Polymer Optical Fibers from a 3D Printer. *Opt. Express* **2018**, *26* (24), 32007.
- Loke, G.; Yan, W.; Khudiyev, T.; Noel, G.; Fink, Y. Recent Progress and Perspectives of Thermally Drawn Multimaterial Fiber Electronics. *Adv. Mater.* **2020**, *32* (1), No. e1904911.
- He, H. X.; Li, C. Z.; Tao, N. J. Conductance of Polymer Nanowires Fabricated by a Combined Electrodeposition and Mechanical Break Junction Method. *Appl. Phys. Lett.* **2001**, *78* (6), 811–813.
- Yang, J.; Keller, M. W.; Moore, J. S.; White, S. R.; Sottos, N. R. Microencapsulation of Isocyanates for Self-Healing Polymers. *Macromolecules* **2008**, *41* (24), 9650–9655.
- Karunaratna, M. H. J. S.; Kim, D.; Parulski-Seager, D. C.; Cho, S.; Mendoza, V.; Han, Y.; Getachew, B. A. Reactivity and Release of Isocyanates from Microcapsules Used in Self-Healing Materials. *Environ. Sci. Technol. Lett.* **2022**, *9* (11), 949–954.
- Hyuk Im, S.; Jeong, U.; Xia, Y. Polymer Hollow Particles with Controllable Holes in Their Surfaces. *Nat. Mater.* **2005**, *4* (9), 671–675.
- Na, J. Y.; Kang, B.; Lee, S. G.; Cho, K.; Park, Y. D. Surface-Mediated Solidification of a Semiconducting Polymer during Time-Controlled Spin-Coating. *ACS Appl. Mater. Interfaces* **2017**, *9* (11), 9871–9879.
- Sultan, M.; Zia, K. M.; Bhatti, H. N.; Jamil, T.; Hussain, R.; Zuber, M. Modification of Cellulosic Fiber with Polyurethane Acrylate Copolymers. Part I: Physicochemical Properties. *Carbohydr. Polym.* **2012**, *87* (1), 397–404.
- Smith, B. C. Organic Nitrogen Compounds III: Secondary and Tertiary Amines. *Spectroscopy* **2019**, *34* (5), 22–26.
- Kumar, N.; Gupta, P. K.; Khilari, S.; Ranganath, K. V. S. Synthesis, Characterization and Catalytic Application of Functionalized Polyureas. *J. Polym. Res.* **2023**, *30* (3), 104.
- Bevas, C. J.; Abel, M.; Jacobs, I.; Watts, J. F. An Interfacial Chemistry Study of Methylene Diphenyl Diisocyanate and Tantalum for Heat Exchanger Applications. *Surf. Interface Anal.* **2020**, *52* (11), 685–693.